HHS Public Access

Author manuscript

Nat Chem Biol. Author manuscript; available in PMC 2017 January 04.

Published in final edited form as:

Nat Chem Biol. 2016 September ; 12(9): 686–693. doi:10.1038/nchembio.2119.

ZDHHC7-Mediated S-Palmitoylation of Scribble Regulates Cell Polarity

Baoen Chen, **Baohui Zheng**, **Micael DeRan**, **Gopala K. Jarugumilli**, **Jianjun Fu**, **Yang S. Brooks**, and **Xu Wu***

Cutaneous Biology Research Center, Massachusetts General Hospital, Harvard Medical School, Charlestown, MA 02129

Abstract

Scribble (SCRIB) is a tumor suppressor protein, playing critical roles in establishing and maintaining epithelial cell polarity. Paradoxically, SCRIB is frequently amplified in human cancers, however, fails to localize properly to cell-cell junctions, suggesting that mislocalization of SCRIB contributes to tumorigenesis. Using chemical reporters, here we showed that SCRIB localization is regulated by S-palmitoylation at conserved cysteine residues. The palmitoylation-deficient mutants of SCRIB are mislocalized, leading to disruption of cell polarity and loss of their tumor suppressive activities to oncogenic YAP, MAPK and PI3K/Akt pathways. We further found that ZDHHC7 is the major palmitoyl acyltransferase regulating SCRIB. Knockout of ZDHHC7 led to SCRIB mislocalization and YAP activation, and disruption of SCRIB's suppressive activities in $HRas^{V12}$-induced cell invasion. In summary, we demonstrated that ZDHHC7-mediated SCRIB palmitoylation is critical for SCRIB membrane targeting, cell polarity, and tumor suppression, providing new mechanistic insights of how dynamic protein palmitoylation regulates cell polarity and tumorigenesis.

The apical-basal polarity of epithelial cells plays critical roles in regulating epithelial cell functions, including migration, proliferation, and apoptosis, and is essential for normal development and tissue homeostasis. Loss of cell polarity leads to tissue disorganization, uncontrolled proliferation and migration, which are hallmarks of epithelial cancers[1]. Cell polarity is tightly regulated by the orchestration of three major conserved protein complexes, including PAR, Crumbs (CRB) and SCRIB complexes[1]. SCRIB is identified as a cell junction localized protein, essential for embryonic polarization and tumor suppression in

*To whom the correspondence should be addressed xwu@cbrc2.mgh.harvard.edu.

Author Contribution

X.W. conceived the concept and supervised the project. B.C. and X.W. designed the experiments. B.Z. and G.J. synthesized the probes, and B.Z. identified Scribble from proteomic studies. B.C. performed biochemistry and cell biology experiments with the help from M.D., G.J., J.F., and Y.B. B.C. and X.W. wrote the paper. All authors discussed the results and commented on the manuscript.

Competing financial interests

The authors declare no competing financial interests.

Additional information

Any supplementary information, chemical compound information and source data are available in the online version of the paper.

Drosophila[2,3]. In addition, overexpression of SCRIB in mammary epithelial cells suppresses epithelial mesenchymal transition (EMT) and promotes epithelial differentiation[4]. Loss of SCRIB disrupts epithelial cell polarity, and contributes to mammary tumorgensis[5], suggesting that SCRIB is a tumor suppressor in mammals. Surprisingly, SCRIB is frequently amplified and overexpressed in multiple human cancers[1,6], opposing its tumor suppressive functions in genetic studies. It has been suggested that proper membrane localization of SCRIB is essential for its tumor suppressive activities, as flies with mislocalized SCRIB mutant phenocopy the SCRIB-deficient mutant. Overexpression of mislocalized SCRIB mutant promotes mammary tumorigenesis by disrupting PTEN functions and activating mTORC1/Akt/S6K pathway[7]. In addition, MAPK pathway is also upregulated by mislocalized SCRIB[4,8,9]. Furthermore, SCRIB is involved in the regulation of the Hippo pathway in breast cancer cells, and mislocalized SCRIB activates YAP/TAZ by antagonizing Hippo signaling[10]. In LKB1-deficient cancers, mislocalized SCRIB inhibits Hippo pathway kinases, leading to YAP nuclear accumulation[11]. Taken together, SCRIB membrane localization could serve as a molecular switch, regulating its tumor suppressive vs. oncogenic functions. Therefore, understanding the mechanisms regulating SCRIB localization will provide new therapeutic opportunities for cancers.

SCRIB is a member of the LAP (LRR and PDZ-containing) family proteins, including Densin-180, ERBIN, Lano and *C. elegans* Let-413[12], which are involved in cell-cell junction regulations. SCRIB contains 16 leucine-rich repeats (LRRs) at N-terminus, followed by two LAP-specific domains (LAPSD) and four PSD-95/Dlg/ZO-1 (PDZ) domains[2]. In *Drosophila*, LRRs are necessary and sufficient to control epithelial cell polarity and proliferation by targeting SCRIB to the plasma membrane[13]. LRR motifs of SCRIB have been identified as a major determinant in the process of membrane targeting, such as binding to E-cadherin[14]. Human SCRIB is mislocalized to cytoplasm when a conserved Pro305 within the LRR region is mutated to leucine (P305L)[15], although this mutant has not been found in any pathological conditions.

Protein S-palmitoylation is a post-translational lipidation by forming a reversible thioester bond between a cysteine residue and 16-carbon fatty acid, palmitate. Palmitoylation plays important roles in regulating trafficking and localization of many peripheral and integral membrane proteins[16]. Previously, we have utilized chemical probes to detect potential palmitoyl acyltransferases and palmitoylated protein using the bioorthogonal chemical reporters[17,18]. Mass spectrometry data revealed that SCRIB is labeled by reversible and irreversible chemical reporters of palmitoylation. Through sequence alignments and site-directed mutagenesis studies, we identified that SCRIB is palmitoylated at two conserved membrane-proximal cysteine residues. Immunofluorescence and confocal microscopy studies showed that palmitoylation of SCRIB is required for its plasma membrane targeting, establishment of epithelial cell polarity and activation of Hippo signaling pathway. We further demonstrated that ZDHHC7 is a major palmitoyl acyltransferase regulating SCRIB, its localization and tumor suppressive functions, revealing new tumor suppressive functions of palmitoyl acyltransferases.

RESULTS

SCRIB is S-Palmitoylated at conserved cysteine residues

To identify potential palmitoylating enzymes or palmitoylated proteins, large-scale proteomic profiling of fatty acylated proteins in the HEK293A cells has been performed using reversible (15-hexadecynoic acid, **1**) or activity-based, irreversible chemical reporter (2-bromohexadec-15-ynoic acid, **2**, Supplementary Results, Supplementary Fig. 1a), followed by copper-mediated 1,3-dipolar cycloaddition (Click reaction) with biotin-azide, enriched by streptavidin beads, and subjected for proteomic analysis by mass spectrometry [19]. The mass spectrometry data suggested both probes could label endogenous SCRIB (Supplementary Fig. 1a). These results are consistent with previous proteomic studies using chemical reporters of palmitoylation[20–25], where SCRIB is among the hits of cellular palmitoylated proteomes. Taken together, the proteomic studies have suggest that SCRIB could be palmitoylated, but detailed biochemical follow-up studies are needed to validate these findings.

Therefore, we set out to confirm that SCRIB could indeed be palmitoylated. We transfected HEK293A cells with N-terminal Flag-tagged SCRIB, labeled cells with 50 μM of **1,** followed by Click reaction with biotin-azide. The streptavidin blot showed that SCRIB could indeed be labeled by **1** (Fig. 1a). In addition, C-terminal EGFP-tagged SCRIB could also be labeled by **1** in HEK293A cells (Supplementary Fig. 1b). Treatment of Click reaction products with 2.5% (v/v) hydroxylamine (NH_2OH) dramatically decreased palmitoylation levels of SCRIB, whereas the labeling by irreversible probe **2** was stable and hydroxylamine-resistant (Fig. 1b, Supplementary Fig. 1c). Taken together, our results confirmed that SCRIB is S-palmitoylated through labile thioester bonds with cysteine residues. To test whether endogenous SCRIB can be palmitoylated, HEK293A cells were metabolically labeled with 100 μM **1** or 50 μM **2**, followed by Click reaction with biotin-azide. The palmitoylated proteome was then enriched by streptavidin beads pull-down. Western blotting for SCRIB in the pull-down samples indicated that endogenous SCRIB was indeed palmitoylated (Fig. 1c, Supplementary Fig. 1d).

To identify the potential palmitoylation site(s) of SCRIB, we aligned the sequences of SCRIB protein across different species, and found three evolutionarily conserved cysteine residues (Cys4, Cys10 and Cys22) at the N-terminus of SCRIB (Supplementary Fig. 1e). These Cys residues are also conserved in other LAP family members, including *C. elegans* LET-413, human Erbin, Densin-180 and Lano (Supplementary Fig. 1e). Interestingly, a previous report suggested that Cys4 and Cys22 could be potential sites of palmitoylation using proteomics-based approaches [25]. We speculate that Cys 4, 10 and/or 22 might be the potential palmitoylation sites, and constructed a series of SCRIB mutants, in which the three cysteines were mutated to serines, singly or in combination. HEK293A cells were transfected with C-terminal EGFP-tagged WT SCRIB or the mutant constructs (single mutant: C4S, C10S, C22S; double mutant: C4/10S, C4/22S, C10/22S; or triple mutant: C4/10/22S), and metabolically labeled with **1**. Streptavidin blot revealed that the mutation of Cys4, Cys10 or both could completely abolish SCRIB palmitoylation, whereas the mutation of Cys22 had little effect (Fig. 1d). These results suggested that the two membrane-proximal

residues (Cys4 and Cys10) are required for SCRIB palmitoylation, and might cooperate with each other for palmitoylation. The P305L mutation of SCRIB has been shown to disrupt its membrane targeting, although the mechanism is not clear[5,15]. Interestingly, although the P305L mutant was expressed at very similar levels with WT SCRIB (the last two lanes of the blot), the palmitoylation levels of this mutant were still much lower than WT SCRIB (Fig. 1d).

We speculate that SCRIB may undergo cycles of palmitoylation and depalmitoylation. To determine the rates of palmitoylation cycling of SCRIB, pulse-chase experiments were performed [26]. Results of multiple pulse-chase experiments showed that the half-life of the palmitoylation turnover of SCRIB is around 27 min, while the protein remained stable during the assay period (Fig. 1e, Supplementary Fig. 1f), suggesting that SCRIB palmitoylation is a dynamic process. Consistently, treatment with 50 μM palmostatin B notably increased SCRIB palmitoylation (Supplementary Fig. 2), indicating that APT1/APT2 might be the depalmitoylating enzyme(s) regulating SCRIB.

Palmitoylation of SCRIB regulates acinar morphogenesis

Madin-Darby canine kidney (MDCK) and MCF10A are two commonly used non-transformed epithelial cell lines. To further explore the roles of SCRIB palmitoylation, we generated MDCK and MCF10A cell lines stably expressing Flag-tagged WT, C4/10S or P305L mutant of SCRIB. Western blot analysis confirmed the comparable expression levels of SCRIB WT and mutant proteins in MDCK (Supplementary Fig. 3a) and MCF10A (Supplementary Fig. 3b) stable cell lines. Confocal immunofluorescent imaging of Flag-SCRIB and cell junction marker ZO-1 protein in MDCK cells showed that SCRIB WT is mainly localized at the cell-cell junctions, whereas the palmitoylation-deficient SCRIB mutant (C4/10S or P305L) showed diffused cytoplasmic localization with similar SCRIB expression levels in these images (Fig. 2a–b).

When cultured at three-dimensional (3D) conditions, the MCF10A mammary epithelial cells form polarized, acini-like spheroids that recapitulate many features of glandular architecture *in vivo*[27]. We next tested whether SCRIB palmitoylation contributes to its localization in 3D culture conditions. MCF10A cells stably expressing SCRIB WT and the mutants were grown on Matrigel for 8 days, followed by immunofluorescent staining and confocal imaging. Consistently, WT SCRIB displayed clear junctional localization in 3D acini, whereas both of the palmitoylation-deficient SCRIB mutants (C4/10S and P305L) showed diffused localization (Fig. 2c, Supplementary Fig. 4). The percentage of acini with mislocalized SCRIB was quantified in these cell lines (Fig. 2d). These results suggested that palmitoylation of SCRIB could regulate SCRIB membrane localization under monolayer or 3D culture conditions.

As SCRIB was known as a major regulator of epithelial cell polarity[1], we next asked whether palmitoylation of SCRIB is required for the establishment of polarized and normal acinar morphogenesis. We cultured MCF10A cells stably expressing SCRIB WT or the palmitoylation-deficient mutants under 3D culture conditions for 14 days to form polarized acini structures, followed by immunostaining with GM130 antibody (an apically localized Golgi marker, showing apical polarity) and α6-integrin antibody (strong basal with weaker

lateral staining, showing basal polarity). In acini expressing palmitoylation-deficient mutants (C4/10S or P305L), the orientation of Golgi apparatus was disrupted in some cells, especially in the cells in the luminal cavity, which was rarely observed in control or acini expressing WT SCRIB (Fig. 2e, Supplementary Fig. 5). The cells expressing WT SCRIB or vector control displayed normal basal polarity (α6-integrin), but loss of the normal acinar morphology and α6-integrin staining at the outer edge of the acini were observed in acini expressing palmitoylation-deficient mutants (Fig. 2f). Luminal filling was quantified by calculating the percentage of filled acini, which contain three or more cells in the luminal cavity. At day 14, acini expressing SCRIB C4/10S or P305L mutant displayed more filled lumen (62% and 64%, respectively) than vector control acini (41%) or WT SCRIB expressing acini (43%) (Fig. 2g), suggesting that expression of palmitoylation-deficient mutants, but not WT SCRIB, prevented luminal clearance during morphogenesis, consistent with pervious studies[5,28]. The acini size at day 14 was also quantified. The average size of acini expressing WT SCRIB is slightly smaller, but not statistically significant, than the vector control or acini expressing the mutants (Supplementary Fig. 6). In summary, WT SCRIB expressing acini showed well-developed lumen structures and normal apical-basal polarity. However, acini expressing the palmitoylation-deficient mutants (C4/10S or P305L) have disrupted lumen structures and partial loss of cell polarity, consistent with a previous study in which SCRIB P305L mutant disrupted acinar morphogenesis[5].

Palmitoylation of SCRIB suppresses oncogenic pathways

Hippo pathway plays critical roles in organ size control and tumor suppression [29]. The major downstream effectors of the Hippo signaling, YAP and TAZ, are transcriptional coactivators, which shuttle between nucleus and cytoplasm[30]. YAP and TAZ can be phosphorylated by the Hippo kinase cascade and sequestered to the cytoplasm. When the Hippo pathway is inactivated, unphosphorylated YAP and TAZ accumulate in the nucleus and regulate the expression of target genes[29]. Recent studies showed that SCRIB is an important upstream regulator of Hippo pathway and suppressor of oncogenic YAP/TAZ in cancer cells[10,11,31]. Next, we investigated whether palmitoylation of SCRIB could affect Hippo signaling and YAP activities. We transfected HEK293A cells with a YAP-responsive reporter (TEAD-binding element driven luciferase reporter, 8xGTIIC-Luc), together with pEGFP-N1 vector control, EGFP-SCRIB WT or palmitoylation-deficient mutants. We found that the suppressive effects of WT SCRIB on YAP reporter activity is statistically significant, while SCRIB mutant (C4/10S or P305L) lost its YAP-suppressive activities (Fig. 3a). Similar levels of EGFP signals indicated comparable expression levels of WT SCRIB and the mutants in the same assay (Fig. 3a). Consistently, expression of WT SCRIB in HEK293A cells, but not the palmitoylation-deficient mutant of SCRIB (C4/10S or P305L), led to increased YAP phosphorylation (p-YAP, S127) levels (Fig. 3b), suggesting that SCRIB palmitoylation is required for its activities in modulating Hippo pathway and suppressing YAP. In addition, we evaluated expression levels of YAP target genes (*CTGF* and *CYR61*) by qRT-PCR in MCF10A and HEK293A cells, with the expression of WT or SCRIB mutant (C4/10S or P305L). Our results showed that expressing of WT SCRIB inhibited YAP target gene expression, while the palmitoylation-deficient mutants lost their inhibitory activities in both cell lines (Fig. 3c, Supplementary Fig. 7). As Hippo pathway-mediated YAP phosphorylation leads to YAP cytoplasmic retention, we next investigated whether SCRIB

palmitoylation can affect YAP localization. We performed confocal immunofluorescent imaging by staining Flag-SCRIB (WT or mutants) and YAP in MDCK stable cell lines, and quantified YAP nuclear localization. Consistently, expression of SCRIB WT, but not the SCRIB mutant (C4/10S or P305L), led to YAP cytoplasmic retention (Fig. 3d–e). In addition, co-immunoprecipitation (co-IP) experiments suggested that SCRIB mutant (C4/10S or P305L) did not affect SCRIB-YAP interaction (Supplementary Fig. 8). Taken together, these results indicate that palmitoylation of SCRIB is involved in the regulation of Hippo signaling pathway, and suppression of YAP activities.

Previous studies showed that SCRIB was also involved in the regulation of MAPK [8,9,28] and PI3K/AKT pathways[7,32]. We asked whether SCRIB palmitoylation-deficient mutants could affect these pathways. MCF10A stable cell lines expressing WT SCRIB or the mutants were incubated for 24 hours without EGF, and then stimulated with 20 ng/mL EGF for the indicated time. In contrast to the WT SCRIB, the palmitoylation-deficient mutant of SCRIB (C4/10S or P305L) did not suppress the phosphorylation of MEK and AKT upon EGF stimulation (Fig. 3f). The results are consistent with previous studies regarding the regulation of MAPK signaling[28] and PI3K/AKT pathway[7,32] by SCRIB.

ZDHHC7 regulates SCRIB palmitoylation

To identify potential SCRIB palmitoylating enzymes, we co-transfected each of the 23 HA-tagged mouse ZDHHC constructs and Flag-SCRIB into HEK293A cells, and metabolically labeled SCRIB using probe **1** (Supplementary Fig. 9). We found that expression of ZDHHC3 or ZHDDC7 could significantly enhance SCRIB palmitoylation levels, with ZDHHC7 as the most potent inducer (Fig. 4a).

In co-IP experiments, we found that ZDHHC7 could directly interact with exogenous or endogenous SCRIB (Fig. 4b, c). When expressed at higher levels, ZDHHC3 could interact with SCRIB, but the interaction was much weaker than that of ZDHHC7 (Supplementary Fig. 10), suggesting that ZDHHC7 might be the major palmitoyl acyltransferase for SCRIB. Consistently, the catalytically inactive mutant of ZDHHC7 (C160S) failed to enhance SCRIB palmitoylation (Fig. 4d). Next, we tested which domains of SCRIB are required for the interaction with ZDHHC7. We constructed three truncated forms of SCRIB, containing the N-terminal LRR domain ($SCRIB^{1-518}$), N-terminal LRR and LAPSD domains ($SCRIB^{1-724}$), and C-terminal PDZ domains ($SCRIB^{717-1655}$), respectively (Supplementary Fig. 11). We transfected these different forms of SCRIB, together with HA-ZDHHC7 into HEK293A cells, and immunoprecipitated (IP) the complex using anti-HA antibody. We successfully detected full-length, $SCRIB^{1-518,}$ and $SCRIB^{1-724}$, but not $SCRIB^{717-1655}$ in the IP samples, indicating that N-terminal LRR domains are required and sufficient to mediate the interaction (Fig. 4e). In addition, we knocked down hZDHHC7 using pooled siRNAs (SMARTpool from GE healthcare), and found that knocking down ZDHHC7 significantly decreased SCRIB palmitoylation (Supplementary Fig. 12). Furthermore, overexpression of mouse HA-ZDHHC7, but not the mutant (C160S), which are partially resistant to the siRNA targeting human ZDHHC7, could rescue SCRIB palmitoylation (Fig. 4f, Supplementary Fig. 13), confirming that it was loss of ZDHHC7 causing the effects. Taken together, these results suggest that ZDHHC7 is a major palmitoylating enzyme for SCRIB.

A previous study suggested that the P305L mutation affected the local structure of the helicoidal part of the LRR13 region, based on the crystal structure model of the LRR domains[33]. Interestingly, overexpression of ZDHHC7 did not increase palmitoylation levels of SCRIB P305L mutant (Supplementary Fig. 14a). We asked whether P305L mutation or C4/10S mutation disrupts ZDHHC7–SCRIB interactions. Surprisingly, our co-IP results showed that the interaction between ZDHHC7–SCRIB (P305L) increased compared with that of ZDHHC7–SCRIB WT (Supplementary Fig. 14b). We speculate that P305L mutation might alter the folding of the protein, leading to a different ZDHHC7–SCRIB interaction mode. While P305L remains binding to ZDHHC7 through LRR domains, the acyltransfer reaction cannot be completed. The increased ZDHHC7–SCRIB (P305L) interaction might be resulted from the slow release (off-rate) of P305L from ZDHHC7, as P305L cannot be converted to the final product, thus cannot be readily released from the enzyme-substrate complex. Future biochemical and enzymatic studies of these reactions will provide more detailed information. On the contrary, ZDHHC7-SCRIB C4/10S interaction decreased significantly (Supplementary Fig. 14b), suggesting that the intact palmitoylation sites are required for the association. These findings are consistent with a previous study demonstrating that ZDHHC7 and ZDHHC21 strongly associate with WT ERα, but fail to interact with ERα C451A mutant[34].

ZDHHC7-mediated palmitoylation regulates SCRIB functions

Next, we investigated whether ZDHHC7 plays important roles in regulating SCRIB membrane targeting and its functions. MCF10A cell lines with stable knockout of ZDHHC7 (KO-1, and KO-2) were generated using CRISPR/Cas9 genome-editing system, and the knockout efficiencies were confirmed by western blot analysis (Supplementary Fig. 15). SCRIB and YAP localization were evaluated by confocal microscopy. We found that loss of ZDHHC7 led to increased SCRIB mislocalization in MCF10A cells (Fig. 5a–b, Supplementary Fig. 16). In addition, re-introducing the ZDHHC7 WT, but not the catalytically dead C160S mutant, to the knockout cells could partially restore SCRIB membrane localization (Fig. 5c–d, Supplementary Fig. 17). Furthermore, co-staining of SCRIB and β-catenin in ZDHHC7 knockout MCF10A cells revealed that β-catenin was still mainly localized to the cell-cell junction (Supplementary Fig. 18), suggesting that adherens junctions remain intact with ZDHHC7 knockout. These results are consistent with the previous report showing expression of mislocalized SCRIB in MCF10A cells did not perturb membrane-associated β-catenin[28]. Furthermore, knockout of ZDHHC7 in MCF10A cells led to increased YAP nuclear localization (Fig. 5e–f). Notably, the suppressive activities of WT SCRIB on YAP target gene expression (*CTGF* and *CYR61*) were partially reversed by loss of ZDHHC7 in MCF10A cells (Supplementary Fig. 19), confirming that ZDHHC7 plays important roles in regulating SCRIB functions.

SCRIB has been implicated in the regulation of cell invasion, transformation and epithelial-to-mesenchymal transition (EMT) [4,8,28,35]. We then tested whether SCRIB palmitoylation could modulate cell invasion and transformation induced by oncogenic $HRas^{V12}$, using a previously reported Matrigel/collagen I system [8,28]. Western blot analysis showed that the expression levels of $HRas^{V12}$ were comparable in different MCF10A stable cell lines (Supplementary Fig. 20). Acini with invasive protrusions were rarely seen in cells without

HRas^{V12} expression (Fig. 6a), suggesting that HRas^{V12} was required for cell invasion. A significant suppression of HRas^{V12}-induced invasion was observed in acini expressing WT SCRIB, whereas acini expressing SCRIB mutant (C4/10S or P305L) displayed similar invasive protrusions to those in vector control acini (Fig. 6a–b, Supplementary Fig. 21). These results are consistent with a previous study showing overexpression of SCRIB P305L was unable to suppress HRas^{V12}-induced cell invasion[28]. Furthermore, we generated MCF10A cell lines with stable knockout of ZDHHC7 (using CRISPR/Cas9 system), together with SCRIB WT and HRas^{V12} expression. Interestingly, knockout of ZDHHC7 in MCF10A stable cells expressing WT SCRIB promoted cell invasion (Fig. 6c–d, Supplementary Fig. 22). Invasive protrusions were not observed in ZDHHC7 knockout MCF10A acini, without SCRIB or HRas^{V12} expression (Supplementary Fig. 23), confirming that the invasive effects of loss of ZDHHC7 are related to SCRIB/HRas^{V12}. Taken together, our results suggest that palmitoylation of SCRIB is required to suppress HRas^{V12}-induced cell invasion, and ZDHHC7 plays important roles in regulating this process. To evaluate the effects of SCRIB palmitoylation in cell transformation, we carried out soft agar colony formation assay. Cells without HRas^{V12} expression formed very few colonies (Supplementary Fig. 24a), confirming that HRas^{V12} was required for anchorage-independent cell growth. Compared with HRas^{V12}-pBABE cells, inhibition of colony formation was observed in all the HRas^{V12}-SCRIB cells, but HRas^{V12}-SCRIB WT cells displayed only slightly stronger suppression than HRas^{V12}-SCRIB (C4/10S or P305L) mutant cells (Supplementary Fig. 24a–b). These findings are consistent with the previous report that WT SCRIB and P305L mutant could suppress anchorage-independent cell growth similarly [28].

A survey of The Cancer Genome Atlas (TCGA) database revealed that SCRIB is frequently amplified in breast and ovarian cancers, and ZDHHC7 is frequently deleted in cancers (such as in Chromosome 16q loss in breast cancers)[36]. According to cancer gene expression database (BioGPS, NCI60 on U133A, gcrma), SCRIB is highly expressed in human ovarian carcinoma cell line OVCAR8. We carried out immunostaining assays, and found that SCRIB is mislocalized in OVCAR8 cells (Supplementary Fig. 25a). We set out to test whether overexpression of ZDHHC7 might promote SCRIB membrane localization in these cancer cells. We transfected OVCAR8 cells with vector control, WT or the catalytically inactive mutant (C160S) of ZDHHC7, and carried out confocal immunofluorescent imaging assays. Interestingly, expression of WT ZDHHC7 notably decreased mislocalized SCRIB, while the catalytic dead mutant ZDHHC7 (C160S) has little effects (Supplementary Fig. 25a–b). In addition, expression of the WT, but not the catalytic dead mutant of ZDHHC7 (C160S), led to increased SCRIB palmitoylation in OVCAR8 cells (Supplementary Fig. 26). Furthermore, expression of WT ZDHHC7, but not the C160S mutant could inhibit OVCAR8 cell proliferation in EdU incorporation assays, suggesting that rescuing SCRIB palmitoylation could inhibit cancer cell proliferation (Supplementary Fig. 27). SCRIB is often amplified, but mislocalized in multiple advanced human cancers, such as breast, ovarian and prostate cancers[1] (Supplementary Fig. 28 and 29), and mislocalization of SCRIB contributes to tumorigenesis[5–7]. Interestingly, ZDHHC7 is frequently deleted in prostate, ovarian and other cancers (Supplementary Fig. 30 and 31), therefore, loss of ZDHHC7 in cancers might contribute to SCRIB depalmitoylation and mislocalization in cancers. Taken together, our

results suggest that ZDHHC7 plays important roles in regulating SCRIB palmitoylation, localization and its tumor suppressive functions.

DISCUSSION

S-palmitoylation is an important lipid modification of many membrane-associated proteins[16]. Here we showed that palmitoylation of SCRIB on two membrane-proximal cysteine residues is required for its plasma membrane targeting. Palmitoylation-deficient mutants of SCRIB are mislocalized, leading to disruption of epithelial cell polarity. Our results suggest that S-palmitoylation of SCRIB might be a molecular switch modulating SCRIB tumor suppressive vs. oncogenic functions. We showed that loss of SCRIB palmitoylation could induce activation of oncogenic YAP, potentially promoting of tumorigenesis[29,30,37]. In addition, SCRIB palmitoylation-deficient mutants lost the ability to suppress MAPK and PI3K/AKT signaling pathways, which may synergize with the activated YAP to promote tumorigenesis. Furthermore, we found that loss of ZDHHC7 compromised the suppressive activities of WT SCRIB in cell invasion, confirming that ZDHHC7 is important for SCRIB's tumor suppressive functions. Taken together, a signal transduction network involving ZDHHC7, SCRIB palmitoylation and the downstream YAP, MAPK or PI3K/AKT pathways might contribute to tumorigenesis in human cancers with deregulated ZDHHC7 and SCRIB (Supplementary Fig. 32).

It is also noted that other DHHC-family of enzymes, such as ZDHHC3, which shares high sequence homology with ZDHHC7, could also promote SCRIB palmitoylation. However, the interaction between ZDHHC3 and SCRIB is much weaker. Therefore, ZDHHC7 is a major enzyme, but not the only one, regulating SCRIB. ZDHHC7 palmitoylates many other cellular substrates, including sex steroid hormone receptors (estrogen receptors and androgen receptor), thereby regulating their plasma membrane localization and rapid signaling in cells[34]. In addition, ZDHHC7 has been shown to mediate palmitoylation of the death receptor Fas, promoting Fas membrane localization and stability by preventing its lysosomal degradation[38]. Therefore, deletion or down-regulation of ZDHHC7 in cancer cells might lead to misregulation of multiple downstream substrates involved in tumorigenesis, suggesting that ZDHHC7 might be a potential tumor suppressor.

Many S-palmitoylated proteins are regulated by cycles of palmitoylation and depalmitoylation[16,39,40]. SCRIB palmitoylation is indeed a dynamic process, and the half-life of palmitoylated SCRIB is relatively short. Depalmitoylating enzymes, such as acylprotein thioesterases and protein palmitoyl thioesterases could remove palmitate from proteins[39,41]. APT1 and APT2 have been described as thioesterases regulating the acylation cycle of Ras[42–44]. A small molecule inhibitor of APT1 and APT2, palmostatin B, significantly increase palmitoylation of H- and N-Ras[44]. Our results are consistent with a previous report that inhibition of depalmitoylating activities enhanced SCRIB palmitoylation detection in proteomic studies[20]. Taken together, our studies revealed that ZDHHC7 regulates SCRIB palmitoylation, its localization and functions, providing new mechanistic insights of deregulation SCRIB in cancers. Rescuing SCRIB palmitoylation by upregulation of ZDHHC7 or inhibition of APT1/APT2 might be potential therapeutic approaches for many cancer cells with deregulated SCRIB.

ONLINE METHODS

Cloning, cell culture, transfection and infection

Full-length human SCRIB cDNA was obtained from DF/HCC DNA Resource Core, and was subcloned into pCMV-3xFlag, pEGFP-N1 and pBABE vectors. All the mutants were generated by site-directed mutagenesis using the QuickChange II Site-Directed Mutagenesis kit (Agilent) following manufacturer's instructions. HEK293A, Phoenix, MDCK and OVCAR8 cells were obtained from ATCC, and cultured in high-glucose Dulbecco's modified Eagles media (DMEM) (Life technologies) with 10% (v/v) fetal bovine serum (FBS) (Thermo/Hyclone, Waltham, MA). MCF10A cells were cultured in DMEM/F12 with 5% horse serum, 100 ng/mL cholera toxin, 500 ng/mL hydrocortisone, 20 ng/mL EGF, 10 μg/mL insulin and 50 μg/mL penicillin/streptomycin. The 3D culture of MCF10A cells was performed using previously published protocols[45]. Expression constructs were transfected into cells using jetPRIME transfection reagent (Polyplus transfection). Retrovirus was prepared using Phoenix cells. After infection, cells were selected for 2 weeks under puromycin before experiments. None of cell lines used in this paper are listed in the database of commonly misidentified cell lines maintained by ICLAC. All cell lines are free of mycoplasma contamination.

Cell labeling and click reaction

15-hexadecynoic acid (**1**) and 2-bromohexadec-15-ynoic acid (**2**) were synthesized in-house with >98% of purity based on LC/MS analysis. HEK293A cells were transfected with SCRIB expression constructs or empty vector. After 36 hours, cells were washed once with PBS and incubated for 2 hours in DMEM with 10% dialyzed FBS. Then cells were treated with chemical probes or DMSO for 4 hours. Labeled cells were washed three times with cold PBS and lysed with lysis buffer containing 50 mM TEA-HCl, pH7.4, 150 mM NaCl, 1% Triton X-100, 0.1% SDS, 1 mM PMSF and 1x EDTA-free cOmplete protease inhibitor cocktail (Roche). Protein concentration was determined by the BCA method. Click reaction was performed in 100 μL lysis buffer containing 50 μg protein, 100 μM biotin-azide, 1 mM tris(2-carboxyethyl)phosphine hydrochloride (TCEP), 100 μM tris[(1-benzyl-1*H*-1,2,3-triazol-4-yl)methy-l]amine (TBTA) and 1 mM $CuSO_4$ for 1 hour at room temperature. The reactions were terminated by the addition of 20 μL of 6x SDS-sample loading buffer (50 mM Tris-HCl, pH 6.8, 6% SDS, 48% Glycerol, 0.03% Bromphenol Blue, 30 mM EDTA, 9% MeSH). The samples were heated for 5 min at 95 °C before being subjected to SDS-PAGE analysis. For the hydroxylamine treatment assay, 2.5% (v/v) hydroxylamine was added to the sample before adding the sample-loading buffer. To detect endogenous palmitoylated proteins, HEK293A cells were incubated overnight with DMSO or 100 μM of probe **1**. The streptavidin agrose beads (Invitrogen) were used to pull-down the labeled proteins from the Click reaction products. After washing three times with wash buffer, the beads were eluted with elution buffer (6 M Urea, 2 % SDS, 30 mM Biotin). The eluted samples were analyzed by western blot.

Analysis of palmitoylation sites on SCRIB

The EGFP-tagged SCRIB mutants were generated by site-directed mutagenesis using the QuikChange kit (Agilent). HEK293A cells were transfected with pEGFP-N1 vector control,

C-terminal EGFP-tagged wild-type SCRIB-EGFP (WT) construct, or mutant (C4S, C10S, C22S, C4S C10S (C4/10S), C4S C22S (C4/22S), C10S C22S (C10/22S), C4S C10S C22S (C4/10/22S) or P305L) construct. Cells were treated for 4 hours with probe **1**. The cells lysates were reacted with azide-biotin and subjected to SDS-PAGE. Western blotting using streptavidin-HRP (1:5000, Life technologies) was performed to analyze palmitoylated SCRIB.

Mass spectrometry analysis

After Click reaction, proteins were precipitated using methanol. The washed protein pellets were dissolved in resuspension buffer containing 4% (w/v) SDS, 50 mM Tris-HCl, pH 7.4, 150 mM NaCl and 10 mM EDTA. Proteins were diluted with 1 volume of Brij97 buffer (50 mM Tris-HCl, pH 7.4, 150 mM NaCl, 10 mM EDTA, 1% Brij97). Prewashed streptavidin-agrose beads were added to each sample. The protein and beads were incubated for 1.5 hours at room temperature on a rotator. The beads then were washed three times with 0.2 SDS in PBS and once with 250 mM ammonium bicarbonate. The captured proteins were incubated for 40 min in dark with 500 μL 8M urea, 50 μL 500 mM TCEP and 50 μL of 400 mM iodoacetamide and then washed twice with 250 mM ammonium bicarbonate. The samples were directly digested on beads and supernatants were collected for LC-MS/MS analysis as described previously[19].

Immunofluorescent staining and confocal microscopy

Cells were seeded on glass cover slips in 6-well plate. After 48 hours incubation, cells were washed 3 times with PBS and fixed with 4% paraformaldehyde in PBS for 10 min at room temperature. Then fixed cells were washed with PBS and permeablized with 0.1% Triton X-100 at room temperature for 5 min. After blocking, coverslips were incubated for one hour with primary antibody and then washed 3 times with 1% Triton X-100. Alexa Fluor-conjugated secondary antibodies (Life technologies) were used at a 1:5000 dilution in blocking buffer. After washing 3 times with PBS, the cover slips were mounted with VECTASHIELD mounting medium (H-1200, Vector laboratories). Indirect immunofluorescent staining of MCF-10A acini was carried out using previously published protocols[45]. Images were captured by Leica TCS-NT 4D confocal microscope. Z stacks were collected with a spacing of 0.2 μm. Antibody and dilutions used in the studies: anti-FLAG M2 (F1804, Sigma Aldrich, 1:1000), anti-YAP (sc-15407, Santa Cruz, 1:100), anti-SCRIB (sc-11049, Santa Cruz, 1:100), anti-ZDHHC7 (ab138210, Abcam, 1:50), anti-ZO-1 (402200, Invitrogen, 1:100), anti-GM130 (BD Biosciences, 610822, 1:100), anti-α6-integrin (MAB1378, Chemicon, 1:100), anti-β-Catenin (BD Biosciences, 610153, 1:100). The membrane localization of SCRIB is evaluated based on the co-localization of SCRIB staining and membrane proteins (ZO-1 or β-Catenin). In images where co-staining of SCRIB and membrane protein are technically difficult, to characterize SCRIB localization, we analyzed the fluorescence-intensity profile along the z-axis from confocal Z-stacks. The properly localized SCRIB is characterized as sharp Z-stack bands as shown in WT SCRIB staining images. The cells with mislocalized SCRIB displayed diffuse fluorescence-intensity distribution around cell nucleus. When the width of the SCRIB Z-stack band is 2-fold larger than the band of WT SCRIB, it is determined as diffused and mislocalized SCRIB. We quantified the percentage of cells with mislocalized SCRIB (diffused staining) for each cell

line. YAP nuclear localization percentage is quantified based on the co-localization of YAP staining and the nuclear DAPI signal using ImageJ software. More than 200 cells are quantified in at least three independent experiments.

Western blotting analysis

Cells were lysed with RIPA buffer supplemented with protease inhibitors (Roche) and phosphatase inhibitors (Roche). Lysates were denatured by heating for 5 minutes at 95 °C and loaded onto 4–12% Bis-Tris polyacrylamide gel. NuPAGE MOPS or MES running buffer (Invitrogen) was used for the SDS-PAGE. The proteins were subsequently transferred to polyvinylidene fluoride membranes (Millipore). The membranes were blocked and incubated with primary antibodies and secondary HRP-conjugated antibodies, and developed by exposure to film. Antibody and dilutions used in the studies: anti-FLAG M2 (F1804, Sigma Aldrich, 1:5000), anti-HA (H3663, Sigma Aldrich, 1:1000), anti-GFP (sc-9996, Santa Cruz, 1:2000), anti-YAP (AT4556a, Abgent, 1:1000), anti-pYAP (13008S, Cell signaling, 1:1000), anti-SCRIB (sc-11049, Santa Cruz, 1:3000), anti-ZDHHC7 (ab138210, Abcam, 1:500), anti-AKT (4691S, Cell signaling, 1:1000), anti-pAKT(4060S, Cell signaling, 1:1000), anti-MEK(4694S, Cell signaling, 1:1000), anti-pMEK (9154S, Cell signaling, 1:1000), anti-H-Ras (sc-520, Santa Cruz, 1:1000), anti-GAPDH (2118S, Cell signaling, 1:1000), anti-β-actin (ab6276, Abcam, 1:500). Full images of blots are shown in the supplementary information (Supplementary Figs. 33–49)

Luciferase reporter assay

HEK293 cells were transiently co-transfected pEGFP vector, WT SCRIB construct, C4/10S mutant construct or P305L mutant construct with the YAP reporter (8xGTIIC-Luc) and a Renilla luciferase control vector. Luciferase assay was performed 24 hours post-transfection using the Dual Glo Luciferase System (Promega). The luminescence was measured using a Perkin Elmer EnVision Multilabel Reader. The relative luminescence was calculated by dividing firefly to Renilla luminescence and normalized using the control cells. GFP signal was detected to show the similar SCRIB expression level in different cell lines in the same assay.

Co-Immunoprecipitation experiments

To test the physical interactions between SCRIB and ZDHHC7, Flag-SCRIB and HA-ZDHHC7 were co-transfected into HEK293A cells. ZDHHC7-interacting proteins were immunoprecipitated by anti-HA magnetic beads (88836, Thermal Scientific), and SCRIB was detected in the complex by western blot using anti-SCRIB antibody (sc-11049, Santa Cruz, 1:1000). Similarly, SCRIB-interacting proteins were immunoprecipitated by anti-Flag magnetic beads (M8823, Sigma-Aldrich), and ZDHHC7 was detected in the complex by western blot using anti-HA antibody (H3663, Sigma Aldrich, 1:1000). To validate the interactions between endogenous SCRIB and ZDHHC7, HEK293A cells was transfected with HA-ZDHHC7 construct or vector control, and the cell lysate was subjected to immunoprecipitation using anti-HA magnetic beads. Endogenous SCRIB was detected in the IP samples by western blot using anti-SCRIB antibody (sc-11049, Santa Cruz, 1:1000). To determine the domain requirements for SCRIB to interact with ZDHHC7, Flag-SCRIB full-length or truncation mutants and HA- ZDHHC7 were co-transfected into HEK293A

cells. ZDHHC7-interacting proteins were immunoprecipitated by anti-HA magnetic beads (88836, Thermal Scientific), and anti-Flag antibody (F1804, Sigma Aldrich, 1:2000) was used to detect Flag-SCRIB truncations.

EGF stimulation assay

MCF-10A cells in growth media were seeded in 6-well plates at 6×10^4 cells/well. Twenty-four hours later, the media was replaced with EGF-free media. Cells were cultured for 24 hours in the absence of EGF and then treated with pre-warmed (37° C) complete media containing 20 ng/ml EGF. After stimulation for the indicated lengths of time, cells were then washed twice with ice-cold PBS and scraped immediately into ice-cold lysis.

Palmitoylation analysis after knockdown of ZDHHC7

HEK293A cells were transfected with 30 nM siRNA control (scramble) and 30 nM (or 10 nM) siRNA-targeting ZDHHC7 (M-021091-00-0005, GE Dharmacon) by using INTERFERin siRNA transfection reagent (40910, Polyplus-transfection SA). After 24 hours, cells were transfected with 1.0 μg Flag-SCRIB plasmid. Forty-eight hours later, cells were labeled with Probe **1** for 1 hour. HEK293A cells were transfected with 30 nM siRNA-targeting ZDHHC7 or control siRNA. Twenty-four hours later, cells were co-transfected with 1.0 μg Flag-SCRIB plasmid and 0.3μg empty vector, wild-type ZDHHC7 (WT) or the mutant (C160S) construct. After 48 hours incubation, cells were labeled with Probe **1** for 1 hour followed by Click reaction.

Generation of ZDHHC7 knockout stable cell lines

Two different sgRNAs targeting human ZDHHC7 (ZDHHC7 KO1: GCACTTGTAGATGACTTCCC and ZDHHC7 KO2: TGGTAGGGGGCAGTACCCAA) were cloned into pLentiCRISPR v2 (lentiCRISPR v2 was a gift from Feng Zhang's lab). Viruses were produced following the published protocols from Zhang lab. The empty vector pLentiCRISPR v2 was taken as control. Briefly, a 10 cm dish of 80% confluent HEK293T cells was transfected using 10 ug of the transfer plasmid, 5 μg pVSVG, 7.5 μg psPAX2, 500 μL of jetPRIME buffer, and 25 μL of jetPRIME transfection reagent. Media was changed after incubation overnight. After 48 hours, viral supernatants were filtered through a 0.45μm low protein binding membrane (Millipore) and used immediately. Transduction was performed in 6-well plate and selected with 1 μg/mL puromycin for 2 weeks. ZDHHC7 knockout efficiency was analyzed by western blot. The mixed cell populations were used for the experiments.

Generation of ZDHHC7 expression stable cell lines

HA tagged ZDHHC7 or C160S mutant was cloned into pBABE-hygro retroviral vector. Retroviruses were produced in Pheonix packaging cell lines. Transduction of MCF10A stable cells (ZDHHC7 knockout or vector control) was performed in 6-well plate and selected under 100 μg/mL hygromycin B for 3 days. HA-ZDHHC7 expression was analyzed by western blot.

Generation of HRas^{V12} expression stable cell lines

MSCV HRas^{V12} IRES GFP retroviral vector (18780, Addgene) was used to produce retrovirus in Pheonix packaging cells. Transductions of MCF10A stable cell lines (pBABE vector, SCRIB WT, C4/10S or P305L) were performed in 6-well plate. At 24 hours post-transduction, media was changed to MCF10A complete media. After 5 days, protein expression levels were analyzed by western blot.

Matrigel/collagen three-dimensional invasion assay

For Matrigel/collagen 3D invasion assay, 1.0 ml rat-tail collagen type I (354236, BD Biosciences) was neutralized with 125 μL of 10xPBS, 125 μL of 0.1 M NaOH, and 25 μL of 0.1 M HCl. The neutralized collagen type I solution was then mixed with 1.0 mL growth factor-reduced (GFR) Matrigel on ice. The final collagen I concentration was 1.6mg/mL. Each well of 8-well chamber slide was coated with 50 μL of Matrigel/collagen I mixture. Cells were plated onto the Matrigel/collagen mixture at 5,000 cells/well in DMEM/F12 with 2% growth factor reduced Matrigel, 2% horse serum, 100 ng/mL cholera toxin, 500 ng/mL hydrocortisone, 10 μg/mL insulin, 5 ng/ml EGF (cells without HRas^{V12} expression) and 50 μg/mL penicillin/streptomycin. Media was replaced every 4 days. Invasive acini were observed and counted on day 6 with the average taken from 3 experiments. The acini size is measured using ImageJ software. More than 100 acini were analyzed and at least 6 fields were counted per condition.

EdU cell proliferation assay

The cell proliferation assay was performed using Invitrogen Click-iT EdU Imaging kit (C10337, Invitrogen). At 24 hours post transfection, OVCAR8 cells were split and seeded on glass coverslips in 6-well plates. After 24 hours incubation, the cells was treated with10 μM EdU for 16 hours. Then cells were fixed with 4% paraformaldehyde in PBS for 10 min, followed by 0.5% Triton X-100 permeabilization for 20 min at room temperature. After Click reaction for EdU detection, immunofluorescent staining was carried out using anti-HA antibody. Hoechst 33342 was diluted in PBS (1:2000) for DNA staining. Images were captured by Leica TCS-NT 4D confocal microscope and analyzed to determine the percentage of the EdU positive cells. The statistical significance of the data was determined by GraphPad Prism 5.0 software.

Statistical methods

No statistical method was used to predetermine sample size. The experiments were not randomized. For biochemical experiments we performed the experiments at least three independent times. Experiments for which we showed representative images were performed successfully at least 3 independent times. No samples were excluded from the analysis. The investigators were not blinded to allocation during experiments and outcome assessment. All *P* values were determined using two-tailed *t*-tests and statistical significance was set at $P = 0.05$. The variance was similar between groups that we compared.

Supplementary Material

Refer to Web version on PubMed Central for supplementary material.

Acknowledgments

This work was supported by Stewart Rahr–MRA (Melanoma Research Alliance) Young Investigator Award, Research Scholar Award from American Cancer Society (124929-RSG-13-291-01-TBE), and grants from National Institutes of Health (R01CA181537 and R01DK107651-01) to X.W. We appreciate Mr. W.-L. Yan for his generous philanthropic donation to Massachusetts General Hospital to support Y.B.'s training and research. We thank Dr. Masaki Fukata for the expression vectors of DHHC proteins, the Confocal Imaging Core at Cutaneous Biology Research Center of Massachusetts General Hospital, and the Shared Instrumentation Grant that covered the purchase of the microscope (1S10RR027673-01), and the Taplin Mass Spec Core at Harvard Medical School for proteomic studies.

References

1. Martin-Belmonte F, Perez-Moreno M. Epithelial cell polarity, stem cells and cancer. Nat Rev Cancer. 2012; 12:23–38. [PubMed: 22169974]
2. Bilder D, Perrimon N. Localization of apical epithelial determinants by the basolateral PDZ protein Scribble. Nature. 2000; 403:676–80. [PubMed: 10688207]
3. Bilder D, Li M, Perrimon N. Cooperative regulation of cell polarity and growth by Drosophila tumor suppressors. Science. 2000; 289:113–6. [PubMed: 10884224]
4. Elsum IA, Martin C, Humbert PO. Scribble regulates an EMT polarity pathway through modulation of MAPK-ERK signaling to mediate junction formation. J Cell Sci. 2013; 126:3990–9. [PubMed: 23813956]
5. Zhan L, et al. Deregulation of scribble promotes mammary tumorigenesis and reveals a role for cell polarity in carcinoma. Cell. 2008; 135:865–78. [PubMed: 19041750]
6. Pearson HB, et al. SCRIB expression is deregulated in human prostate cancer, and its deficiency in mice promotes prostate neoplasia. J Clin Invest. 2011; 121:4257–67. [PubMed: 21965329]
7. Feigin ME, et al. Mislocalization of the cell polarity protein scribble promotes mammary tumorigenesis and is associated with Basal breast cancer. Cancer Res. 2014; 74:3180–94. [PubMed: 24662921]
8. Dow LE, et al. Loss of human Scribble cooperates with H-Ras to promote cell invasion through deregulation of MAPK signalling. Oncogene. 2008; 27:5988–6001. [PubMed: 18641685]
9. Godde NJ, et al. Scribble modulates the MAPK/Fra1 pathway to disrupt luminal and ductal integrity and suppress tumour formation in the mammary gland. PLoS Genet. 2014; 10:e1004323. [PubMed: 24852022]
10. Cordenonsi M, et al. The Hippo transducer TAZ confers cancer stem cell-related traits on breast cancer cells. Cell. 2011; 147:759–72. [PubMed: 22078877]
11. Mohseni M, et al. A genetic screen identifies an LKB1-MARK signalling axis controlling the Hippo-YAP pathway. Nat Cell Biol. 2014; 16:108–17. [PubMed: 24362629]
12. Santoni MJ, Pontarotti P, Birnbaum D, Borg JP. The LAP family: a phylogenetic point of view. Trends Genet. 2002; 18:494–7. [PubMed: 12350333]
13. Zeitler J, Hsu CP, Dionne H, Bilder D. Domains controlling cell polarity and proliferation in the Drosophila tumor suppressor Scribble. J Cell Biol. 2004; 167:1137–46. [PubMed: 15611336]
14. Navarro C, et al. Junctional recruitment of mammalian Scribble relies on E-cadherin engagement. Oncogene. 2005; 24:4330–9. [PubMed: 15806148]
15. Audebert S, et al. Mammalian Scribble forms a tight complex with the betaPIX exchange factor. Curr Biol. 2004; 14:987–95. [PubMed: 15182672]
16. Linder ME, Deschenes RJ. Palmitoylation: policing protein stability and traffic. Nat Rev Mol Cell Biol. 2007; 8:74–84. [PubMed: 17183362]
17. Hannoush RN, Sun J. The chemical toolbox for monitoring protein fatty acylation and prenylation. Nat Chem Biol. 2010; 6:498–506. [PubMed: 20559317]
18. Hang HC, Linder ME. Exploring protein lipidation with chemical biology. Chem Rev. 2011; 111:6341–58. [PubMed: 21919527]
19. Zheng B, et al. 2-Bromopalmitate analogues as activity-based probes to explore palmitoyl acyltransferases. J Am Chem Soc. 2013; 135:7082–5. [PubMed: 23631516]

20. Martin BR, Wang C, Adibekian A, Tully SE, Cravatt BF. Global profiling of dynamic protein palmitoylation. Nat Methods. 2012; 9:84–9. [PubMed: 22056678]
21. Kang R, et al. Neural palmitoyl-proteomics reveals dynamic synaptic palmitoylation. Nature. 2008; 456:904–9. [PubMed: 19092927]
22. Wei X, Song H, Semenkovich CF. Insulin-regulated protein palmitoylation impacts endothelial cell function. Arterioscler Thromb Vasc Biol. 2014; 34:346–54. [PubMed: 24357059]
23. Martin BR, Cravatt BF. Large-scale profiling of protein palmitoylation in mammalian cells. Nat Methods. 2009; 6:135–8. [PubMed: 19137006]
24. Li Y, Martin BR, Cravatt BF, Hofmann SL. DHHC5 protein palmitoylates flotillin-2 and is rapidly degraded on induction of neuronal differentiation in cultured cells. J Biol Chem. 2012; 287:523–30. [PubMed: 22081607]
25. Yang W, Di Vizio D, Kirchner M, Steen H, Freeman MR. Proteome scale characterization of human S-acylated proteins in lipid raft-enriched and non-raft membranes. Mol Cell Proteomics. 2010; 9:54–70. [PubMed: 19801377]
26. Zhang MM, Tsou LK, Charron G, Raghavan AS, Hang HC. Tandem fluorescence imaging of dynamic S-acylation and protein turnover. Proc Natl Acad Sci U S A. 2010; 107:8627–32. [PubMed: 20421494]
27. O'Brien LE, Zegers MM, Mostov KE. Opinion: Building epithelial architecture: insights from three-dimensional culture models. Nat Rev Mol Cell Biol. 2002; 3:531–7. [PubMed: 12094219]
28. Elsum IA, Humbert PO. Localization, not important in all tumor-suppressing properties: a lesson learnt from scribble. Cells Tissues Organs. 2013; 198:1–11. [PubMed: 23774808]
29. Johnson R, Halder G. The two faces of Hippo: targeting the Hippo pathway for regenerative medicine and cancer treatment. Nat Rev Drug Discov. 2014; 13:63–79. [PubMed: 24336504]
30. Moroishi T, Hansen CG, Guan KL. The emerging roles of YAP and TAZ in cancer. Nat Rev Cancer. 2015; 15:73–9. [PubMed: 25592648]
31. Yang CC, et al. Differential regulation of the Hippo pathway by adherens junctions and apical-basal cell polarity modules. Proc Natl Acad Sci U S A. 2015; 112:1785–90. [PubMed: 25624491]
32. Li X, Yang H, Liu J, Schmidt MD, Gao T. Scribble-mediated membrane targeting of PHLPP1 is required for its negative regulation of Akt. EMBO Rep. 2011; 12:818–24. [PubMed: 21701506]
33. Legouis R, et al. Basolateral targeting by leucine-rich repeat domains in epithelial cells. EMBO Rep. 2003; 4:1096–102. [PubMed: 14578922]
34. Pedram A, Razandi M, Deschenes RJ, Levin ER. DHHC-7 and -21 are palmitoylacyltransferases for sex steroid receptors. Mol Biol Cell. 2012; 23:188–99. [PubMed: 22031296]
35. Vaira V, et al. Aberrant overexpression of the cell polarity module scribble in human cancer. Am J Pathol. 2011; 178:2478–83. [PubMed: 21549346]
36. Hungermann D, et al. Influence of whole arm loss of chromosome 16q on gene expression patterns in oestrogen receptor-positive, invasive breast cancer. J Pathol. 2011; 224:517–28. [PubMed: 21706489]
37. Harvey KF, Zhang X, Thomas DM. The Hippo pathway and human cancer. Nat Rev Cancer. 2013; 13:246–57. [PubMed: 23467301]
38. Rossin A, et al. Fas palmitoylation by the palmitoyl acyltransferase DHHC7 regulates Fas stability. Cell Death Differ. 2015; 22:643–53. [PubMed: 25301068]
39. Fukata Y, Fukata M. Protein palmitoylation in neuronal development and synaptic plasticity. Nat Rev Neurosci. 2010; 11:161–75. [PubMed: 20168314]
40. Rocks O, et al. The palmitoylation machinery is a spatially organizing system for peripheral membrane proteins. Cell. 2010; 141:458–71. [PubMed: 20416930]
41. Wan J, Roth AF, Bailey AO, Davis NG. Palmitoylated proteins: purification and identification. Nat Protoc. 2007; 2:1573–84. [PubMed: 17585299]
42. Duncan JA, Gilman AG. A cytoplasmic acyl-protein thioesterase that removes palmitate from G protein alpha subunits and p21(RAS). J Biol Chem. 1998; 273:15830–7. [PubMed: 9624183]
43. Rocks O, et al. An acylation cycle regulates localization and activity of palmitoylated Ras isoforms. Science. 2005; 307:1746–52. [PubMed: 15705808]

44. Dekker FJ, et al. Small-molecule inhibition of APT1 affects Ras localization and signaling. Nat Chem Biol. 2010; 6:449–56. [PubMed: 20418879]

45. Debnath J, Muthuswamy SK, Brugge JS. Morphogenesis and oncogenesis of MCF-10A mammary epithelial acini grown in three-dimensional basement membrane cultures. Methods. 2003; 30:256–68. [PubMed: 12798140]

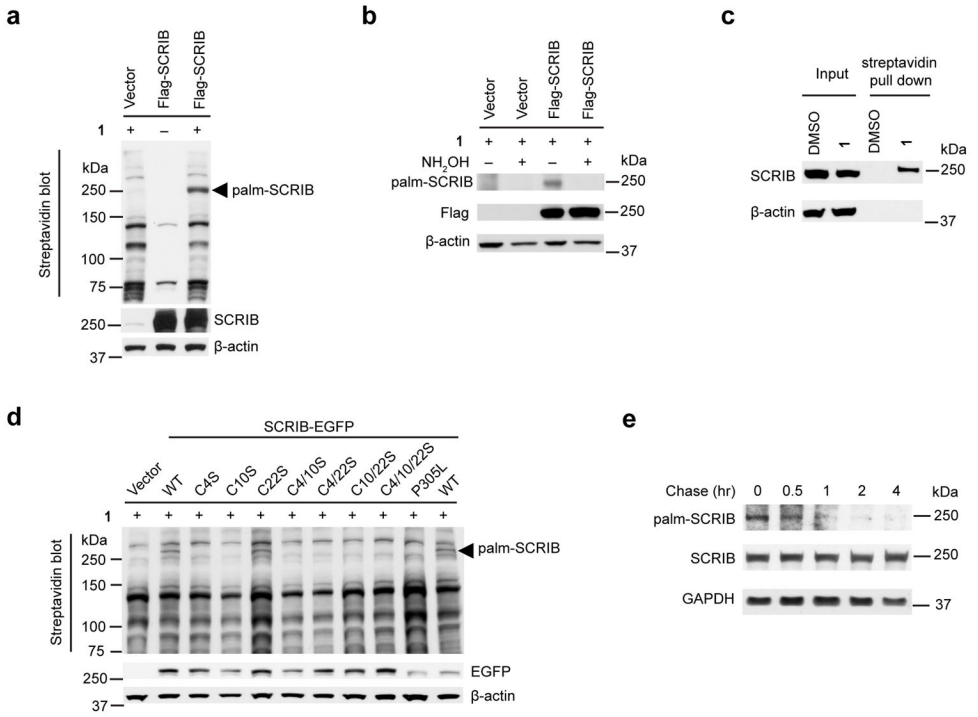

Figure 1. SCRIB is S-palmitoylated at evolutionarily conserved N-terminal cysteine residues

(**a**) Biochemical validation of SCRIB palmitoylation by metabolic labeling using chemical reporters of palmitoylation and streptavidin blot.

(**b**) Treatment with hydroxylamine significantly decreased SCRIB palmitoylation.

(**c**) Streptavidin pull-down and western blotting confirmed that endogenous SCRIB is palmitoylated in HEK293A cells.

(**d**) Mutation of cysteine 4 and/or 10 abolished palmitoylation of SCRIB.

(**e**) Pulse-chase analysis showed dynamic S-palmitoylation of SCRIB.

All blots are representatives of at least three independent experiments.

See Supplementary Figure 33 for full images of the blots in **a–e**.

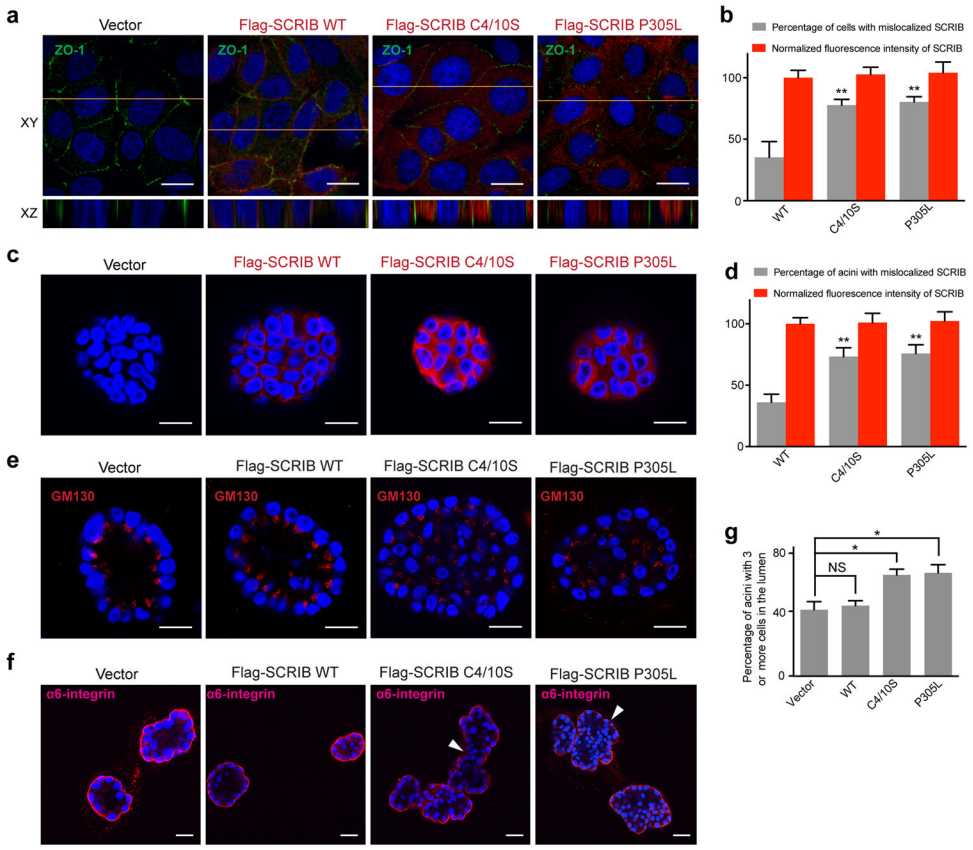

Figure 2. Palmitoylation of SCRIB regulates its membrane localization and epithelial cell polarity

(**a**) SCRIB (C4/10S or P305L) mutant disrupted its membrane localization in MDCK cells. Cells were stained with anti-Flag antibody (red), anti-ZO1 antibody (green), and nuclei (DAPI, blue). The yellow line indicates the position of the Z stack.

(**b**) The percentage of cells with mislocalized SCRIB in MDCK cells were quantified.

(**c**) SCRIB (C4/10S or P305L) mutant were mislocalized in MCF10A acini at day 8 of 3-D culture. Cells were stained with anti-Flag antibody (red) and DAPI (blue).

(**d**) The percentage of acini with mislocalized SCRIB in MCF10A cells were quantified. Expression levels of SCRIB were measured by the fluorescence intensity of SCRIB (in **a**–**d**).

(**e**–**f**) SCRIB (C4/10S or P305L) mutant disrupted the acinar morphogenesis of MCF10A cells at 3-D culture at day 14. Acini were stained with anti-GM130 antibody (red) and DAPI (blue) (**e**), or anti-α6-integrin antibody (red) and DAPI (blue) (**f**).

(**g**) The percentage of MCF10A acini with filled lumen was quantified. SCRIB (C4/10S or P305L) mutant showed increased luminal filling in MCF10A acini.

Scale bars represent 20 μm in all images.

All data are represented as mean ± SEM, n=3. *P* values were determined using two-tailed t-tests. *, $P<0.05$, **, $P<0.005$, N.S., not significant.

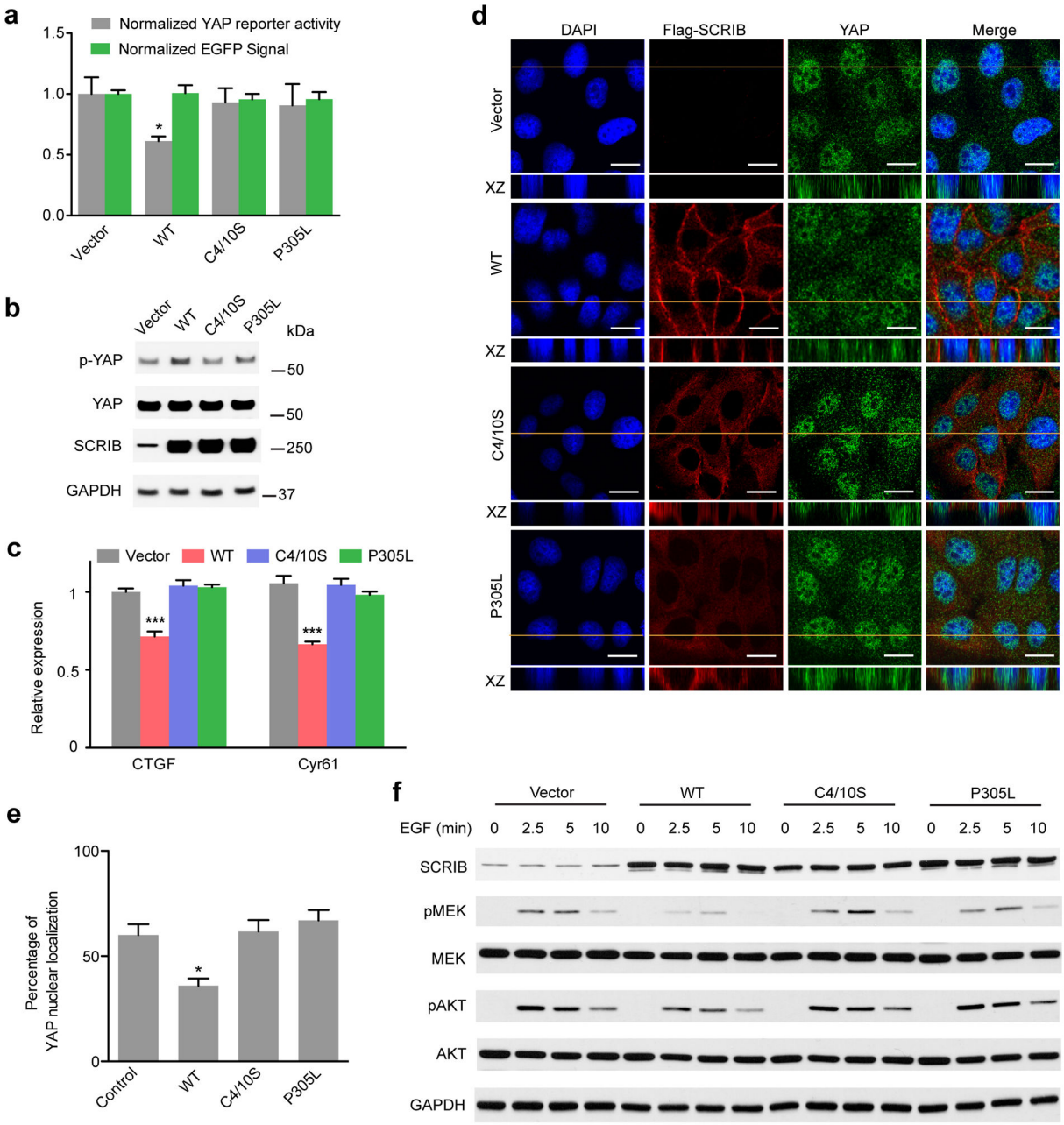

Figure 3. Palmitoylation of SCRIB is required to suppress YAP, MAPK and PI3K/AKT pathways

(**a**) Palmitoylation-deficient mutant of SCRIB (C4/10S or P305L) lost its suppression to YAP reporter (8xGTIIC-Luc) activity. EGFP signal was detected to show the similar SCRIB expression level in different cell lines.

(**b**) Palmitoylation-deficient SCRIB mutant reduced YAP S127 phosphorylation in HEK293A cells. At 36 hours post transfection, cells were harvested for western blot analysis.

(**c**) Palmitoylation-deficient mutant of SCRIB (C4/10S or P305L) lost the suppressive activities of YAP target gene expression (*CTGF* and *Cyr61*) in MCF10A cells. Relative mRNA levels were normalized to vector control.
(**d**) Palmitoylation-deficient mutant of SCRIB (C4/10S or P305L) did not suppress YAP nuclear localization in MDCK cells. MDCK stable cells were stained with anti-Flag antibody (Flag-SCRIB, red), anti-YAP antibody (green) and nuclear DAPI (blue). The yellow line indicates the position of the Z stack. Scale bars represent 20 μm.
(**e**) Quantification of the percentage of YAP nuclear localization in MDCK cells.
(**f**) Palmitoylation-deficient SCRIB mutant (C4/10S or P305L) is not sufficient to suppress EGF-stimulated MAPK and PI3K/AKT pathways activation.
All blots are representatives of at least three independent experiments.
All data are represented as mean ± SEM, n=3. *P* values were determined by two-tailed *t*-test. *, $P<0.05$.***, $P<0.001$.
See Supplementary Figure 34 for full images of the blots in **b** and **f**.

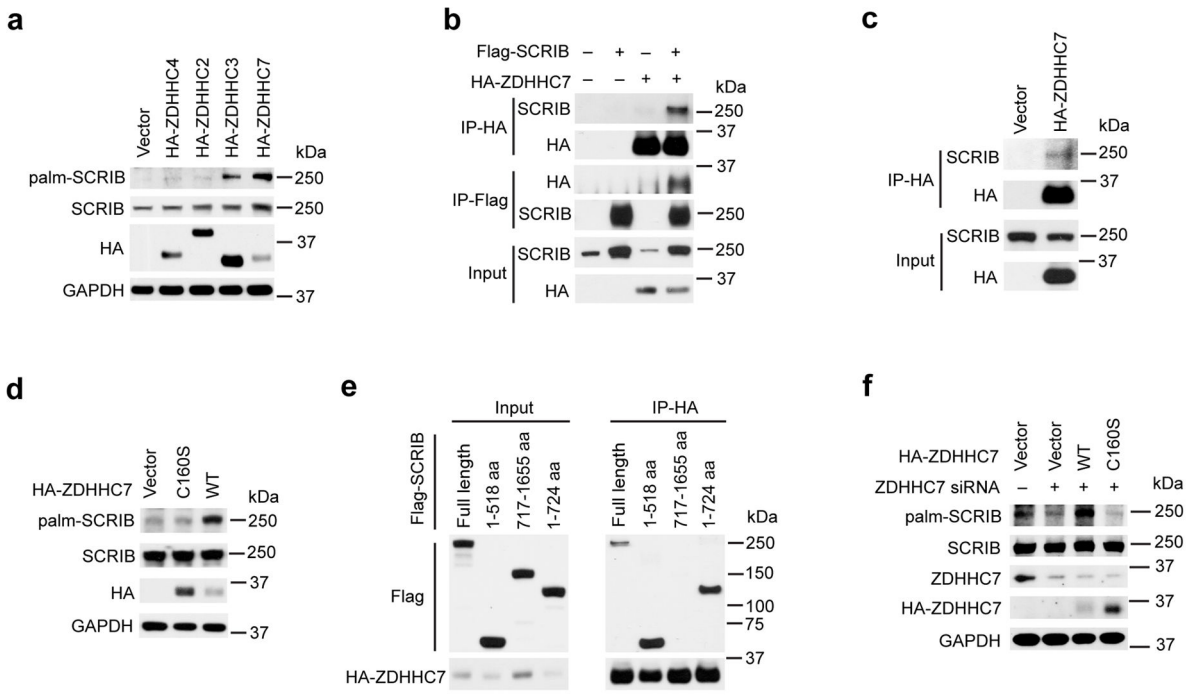

Figure 4. ZDHHC7 is a major palmitoyl acyltransferase regulating SCRIB palmitoylation

(**a**) Overexpression of ZDHHC7 significantly increased SCRIB palmitoylation levels. HEK293A cells were co-transfected with Flag-SCRIB construct and HA-ZDHHC constructs or empty vector.

(**b**) Flag-SCRIB physically interacted with HA-ZDHHC7 in co-immunoprecipitation assays when co-transfected into cells.

(**c**) Endogenous SCRIB interacted with HA-ZDHHC7 in co-immunoprecipitation assays.

(**d**) The catalytic inactive mutant of ZDHHC7 (C160S) failed to induce SCRIB palmitoylation.

(**e**) The N-terminal LRR domains of SCRIB are required and sufficient for ZDHHC7-SCRIB interaction.

(**f**) Expression of siRNA-resistant construct of mouse WT HA-ZDHHC7 rather than the catalytically inactive mutant (C160S) restored SCRIB palmitoylation.

All blots are representatives of at least three independent experiments.

See Supplementary Figure 35 for full images of the blots.

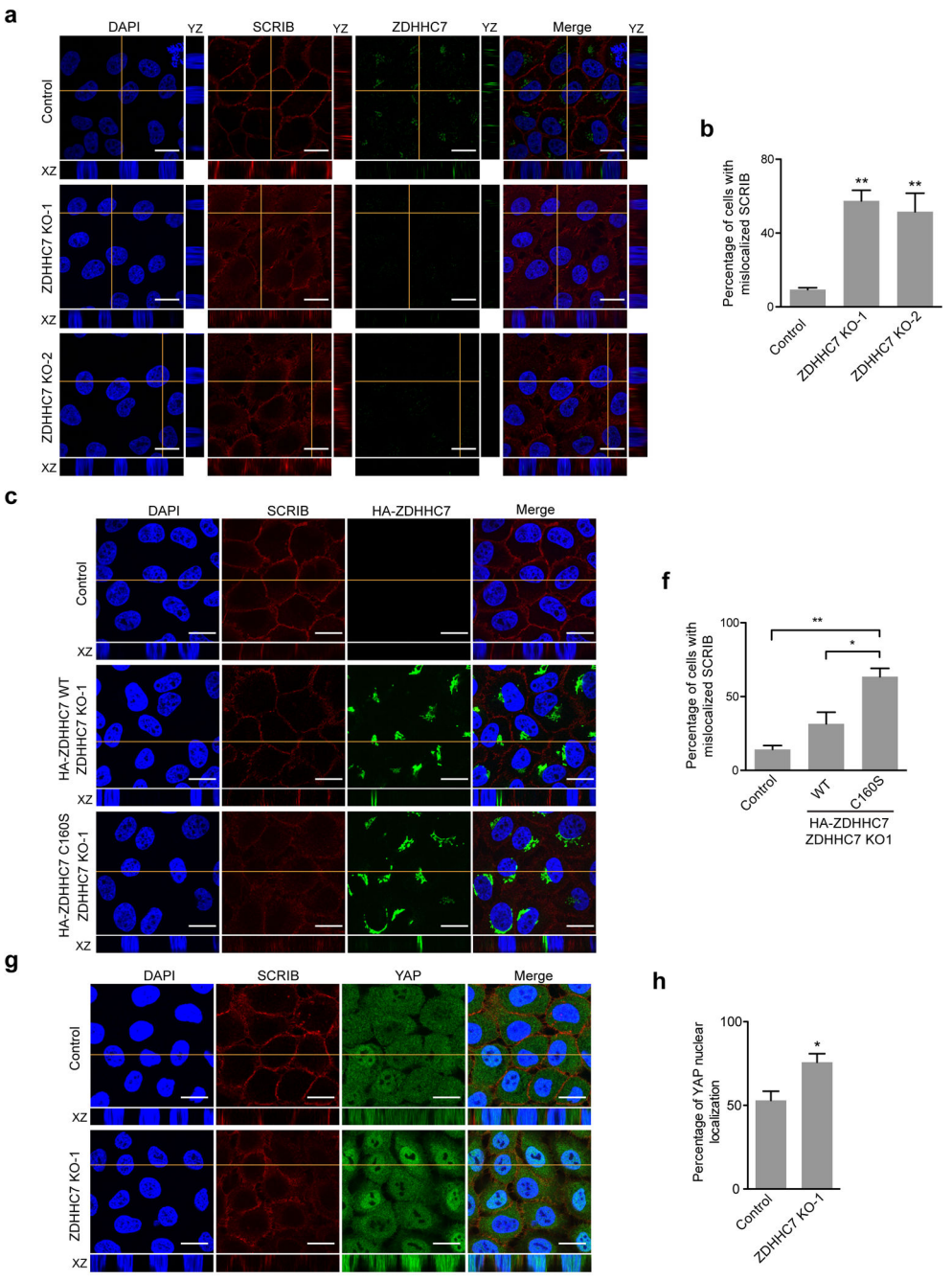

Figure 5. ZDHHC7-mediated palmitoylation regulates SCRIB localization and YAP translocation

(**a**) Knockout of ZDHHC7 in MCF10A cells led to SCRIB mislocalization. Cells were stained with anti-SCRIB antibody (red), anti-ZDHHC7 antibody (green) and DAPI (blue).

(**b**) Quantification of the percentage of cells with mislocalized SCRIB in ZDHHC7 knockout cells.

(**c**) Expression of WT ZDHHC7, but not the C160S mutant partially restored SCRIB membrane localization in ZDHHC7 KO cells. Cells were stained with anti-SCRIB antibody (red), anti-ZDHHC7 antibody (green) and DAPI (blue).

(**d**) Quantification of the percentage of cells with mislocalized SCRIB in different ZDHHC7 knockout cells.
(**e**) Knockout of ZDHHC7 in MCF10A cells led to increased YAP nuclear localization. Cells were stained with anti-SCRIB antibody (red), anti-YAP antibody (green) and DAPI (blue).
(**f**) Quantification of the percentage of YAP nuclear localization in ZDHHC7 knockout cells.
In all images, the yellow line indicates the position of the Z stack (XY or XZ). Scale bars represent 20 μm.
Data are represented as mean ± SEM, n=3. *P* values were determined by two-tailed *t*-test. *, $P<0.05$, **, $P<0.01$.

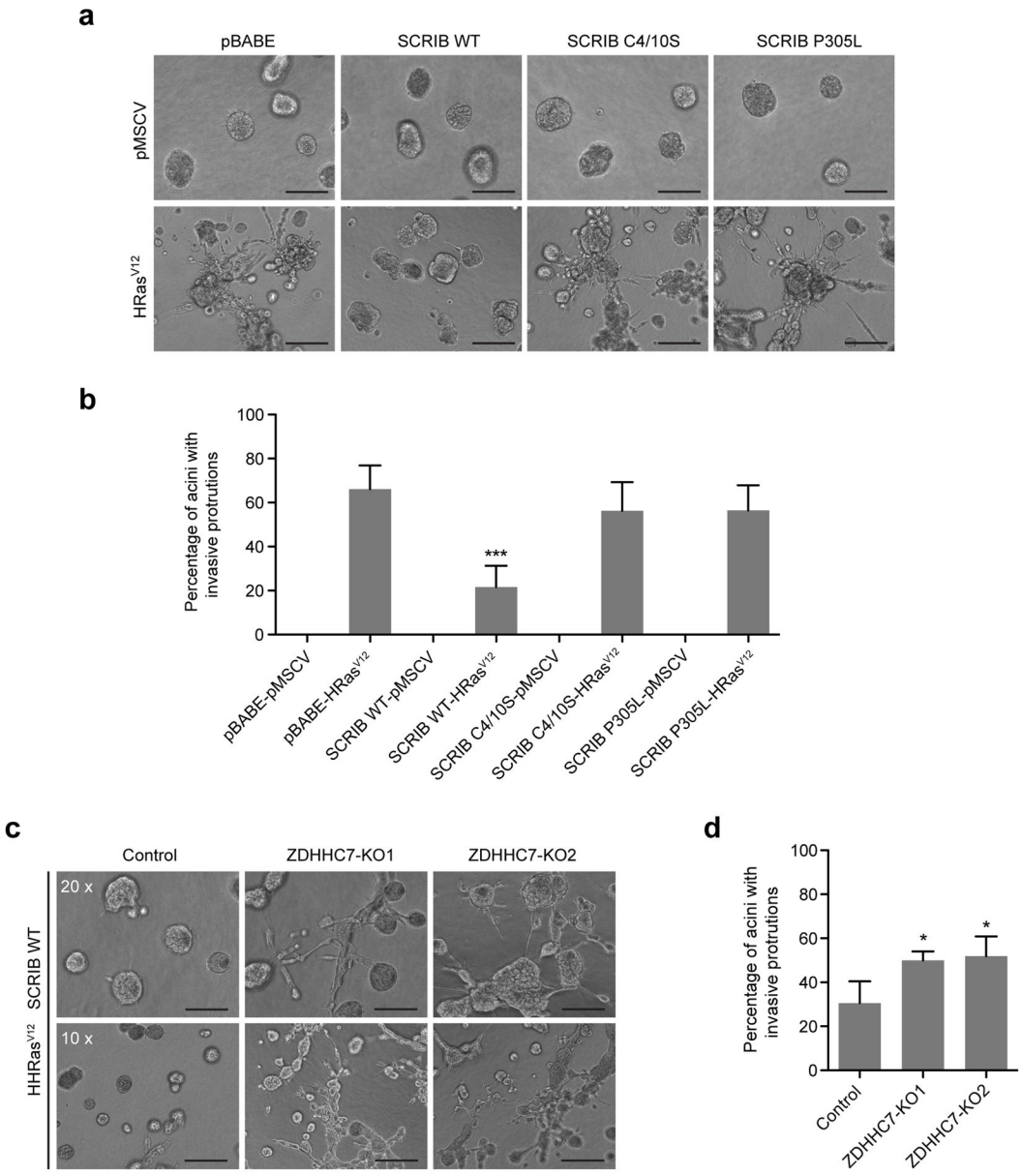

Figure 6. Palmitoylation of SCRIB is required to suppress HRas^{V12}-induced cell invasion

(**a**) Representative images of different MCF10A stable cell lines cultured in Matrigel/collagen mixture for 6 days. Scale bars represent 50 μm.

(**b**) Quantification of the percentage of acini with invasive protrusions in each cell line. At least 100 acini were analyzed for each cell line in three independent experiments.

(**c**) Representative images of control or ZDHHC7-knockout cells cultured in Matrigel/collagen mixture for 6 days. High magnification (upper, 20×) view and low magnification (lower, 10×) view are shown, respectively. Scale bars represent 50 μm, and 100 μm, respectively.

(**d**) Quantification of the percentage of acini with invasive protrusions in vector control and ZDHHC7-knockout MCF10A cells. At least 100 acini were analyzed for each cell line in three independent experiments.

All data are represented as mean ± SEM, n = 6. *P* values were determined by two-tailed *t*-test, compared with the vector control cells. *, $P < 0.05$; ***, $P < 0.001$.